Recovering Latent Causal Factor for Generalization to Distributional Shifts

Xinwei Sun[*1], **Botong Wu**[†2], **Xiangyu Zheng**[†2], **Chang Liu**[1], **Tao Qin**[1], **Wei Chen**[1], **Tie-Yan Liu**[1]
[1] Microsoft Research Asia, Beijing, 100080
[2] Peking University, Beijing, 100871
{xinsun,changliu,wche,taoqin,tyliu}@microsoft.com, botongwu@pku.edu.cn

Abstract

Distributional shifts between training and target domains may degrade the prediction accuracy of learned models, mainly because these models often learn features that possess only correlation rather than causal relation with the output. Such a correlation, which is known as "spurious correlation" statistically, is domain-dependent hence may fail to generalize to unseen domains. To avoid such a spurious correlation, we propose **La**tent **C**ausal **I**nvariance **M**odels (LaCIM) that specifies the underlying causal structure of the data and the source of distributional shifts, guiding us to pursue only causal factor for prediction. Specifically, the LaCIM introduces a pair of correlated latent factors: (a) causal factor and (b) others, while the extent of this correlation is governed by a domain variable that characterizes the distributional shifts. On the basis of this, we prove that the distribution of observed variables conditioning on latent variables is shift-invariant. Equipped with such an invariance, we prove that the causal factor can be recovered without mixing information from others, which induces the ground-truth predicting mechanism. We propose a Variational-Bayesian-based method to learn this invariance for prediction. The utility of our approach is verified by improved generalization to distributional shifts on various real-world data. Our code is freely available at https://github.com/wubotong/LaCIM.

1 Introduction

Current data-driven deep learning models, revolutionary in various tasks though, often exploit all types of correlations to fit data well. Among such correlations, there can be spurious ones corresponding to biases (*e.g.*, confounding bias due to the presence of a third unseen factor) inherited from the data provided. Such data-dependent spurious correlations can erode the prediction power on unseen domains with distributional shifts, which can cause serious consequences especially in safety-critical tasks such as healthcare.

Recently, there is a Renaissance of causality in machine learning, expected to pursue causal relationships [59] to achieve stable generalization across domains. The so-called area of "causality" is pioneered by Structural Causal Models [51], as a mathematical formulation of this metaphysical concept grasped in the human mind. The incorporation of these human priors about cause and effect endows the model with the ability to identify the causal structure [51] which entails not only the data but also the underlying process of how they are generated. To achieve causal modeling, the old-school methods [52, 10] directly causally related the output label Y to a subset of *covariates* X, which is however *not* conceptually reasonable in applications with sensory-level data (*e.g. model pixels as causal factors of the output does not make sense in image classification [11]*).

[*]Corresponding author
[†]Work done during an internship at Microsoft Research Asia.

35th Conference on Neural Information Processing Systems (NeurIPS 2021), Sydney, Australia.

For such applications, we rather adopt the manner of human visual perception [8, 9, 80] to causally relate the label Y to unobserved abstractions denoted by S, *i.e.*, $Y \leftarrow S$. We further assume the existence of another non-causal latent factor (of Y) denoted as Z, that together with S generate the input X: $X \leftarrow (S, Z)$. Such an assumption is similarly adopted in the literature [25, 27, 35, 75, 71]. To model shifts across domains, we allow Z to be spuriously correlated with S (hence also the output), as marked by the bidirected arrow in Fig. 1 (a). Taking image classification as an example, the S and Z respectively refer to object-related abstractions (*e.g.*, contour, texture) and contextual information (*e.g.*, background, view). Due to this correlation, the model can learn contextual information into prediction, which may fail to generalize to the domain such that this correlation is broken.

We encapsulate above assumptions into the skeleton illustrated in Fig. 1 (a), in which the spurious correlation between S and Z varies across domains, as marked by the red bi-directed arrow in Fig. 1 (b). Taking a closer inspection, such a domain-dependent spurious correlation is governed by an auxiliary domain variable D in Fig. 1 (c), which causes the domain shifts. We call the set of causal models augmented with D as **La**tent **C**ausal **I**nvariance **M**odels (LaCIM). Here, the "Causal Invariance" refers to $P(Y|S)$, which together with $P(X|S, Z)$, can be proved to be stable to the shifts across domains, under the assumptions embedded in the causal structure of LaCIM. Equipped with such an invariance, we prove that the S and the ground-truth predictor: $P(Y|s^\star)$ for x generated from $(s^\star, z^\star)$, are identifiable up to transformations that do not mix the non-causal information.

Under such an identifiability guarantee, we propose to learn the $P(Y|S)$ and $P(X|S, Z)$ by reformulating the Variational Auto-encoder (VAE) [37] to fit the joint distribution of the input and output variables from training domains. During the test stage, we first infer the value of S by optimizing the estimated $P(X|S, Z)$ over latent space, followed by the learned $P(Y|S)$ for prediction. We first use simulated data to verify the correctness of the identifiability claim. Then, to demonstrate the utility, we test our approach on real-world data, consistently achieving better generalization to the new distribution; besides, we find that our inferred causal factor can be concentrated in highly explainable semantic regions for the task of image classification.

We summarize our contribution as follows: **Methodologically** (in sec. 4.1), we propose LaCIM in which the causal assumptions of two latent factors and the distributional shifts are incorporated; **Theoretically** (in theorem 4.4), we prove the identifiability of the causal factor and the ground-truth predicting mechanism; **Algorithmically** (in sec. 4.3), guided by the identifiability, we reformulate Variational Bayesian method to learn $P(X|S, Z)$, $P(Y|S)$ for prediction; **Experimentally** (in sec. 5.2), our approach generalizes better to distributional shifts, compared with others.

2 Related Work

Causality for Domain Generalization. Due to its stable transferability, the concept of causality has been introduced in many recent works for domain generalization [39, 59, 52, 10, 40, 21, 68]. Most of these works learned the assumed (causal) invariance for generalizing to unseen domains. However, they suffer from either **i)** lacking explicit causal modeling; or **ii)** inappropriate causal relations made for the output. Specifically, for **i)**, the [39, 59] are still data-driven methods to learn stable correlation (*i.e.*, invariance) without incorporating causal assumptions [51] beyond data, which may impede its generalization to a broader set of domains; for **ii)**, the [52, 10, 40, 21, 68] causally relate the output with covariates, which is inappropriate for sensory-level data.

Our Specification. We explicitly incorporate the causal assumptions. Specifically, we introduce **i)** latent factors and separate them into the causal and the non-causal factor; **ii)** the domain variable D, as a selecting mechanism to generate the varied S-Z correlation across domains. Such a causal modeling makes it possible to recover the causal factor S for generalization. In independent and concurrent works, [75] and [28] also explore latent variables in causal relation. As comparisons, [75] did not differentiate S from Z. The spurious correlation in [28] is limited in the correlation between domains and the output; while it is allowed in our setting to exist in a single domain, which is more aligned with real scenarios, *e.g.*, the dog is more associated with grass than snow in a domain when most samples are collected in sunny morning.

Other Conceptually Related Works: i) transfer learning that leverages invariance in the context of domain adaptation [60, 81, 17] or domain generalization [43, 63]; **(ii)** causal inference [51, 53] which builds structural causal models and define intervention (*a.k.a*, "do-calculus") for cause-effect reasoning and counterfactual learning; and **(iii)** latent generative model that assumes generation from latent space to observed data [37, 71] *but* aims at learning generator in the unsupervised scenario.

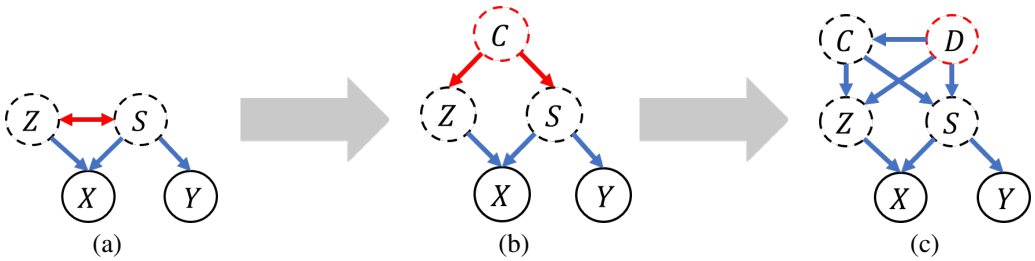

Figure 1: The introduction of *Latent Causal Invariant Models*, a set of SCMs augmented with a domain variable D in (c), starting from the skeleton in (a). Specifically, from (a) to (b): the spurious correlation between S and Z is due to an unobserved confounder C, with distributional shifts referring to change of $P(C)$ and $P(S, Z|C)$ across domains; from (b) to (c): we ascribe such shifts to the domain variable D, as the source of distributional shifts. Here, the observed and unobserved variables are respectively marked by solid and dot circles; the directed arrow ("$\rightarrow$" or "$\leftarrow$") represents direct causal relation; while the bidirected arrows ("$\leftrightarrow$") represent the spurious correlation that can vary across domains; the red and blue respectively means the invariant and varied values/distributions.

3 Preliminaries

Problem Setting. Let X, Y respectively denote the input and output variables. The training data $\{\mathcal{D}^e\}_{e\in\mathcal{E}_{\text{train}}}$ are collected from multiple environments $e \in \mathcal{E}_{\text{train}}$, where each e is associated with a distribution $\mathrm{P}^e(X, Y)$ over $\mathcal{X} \times \mathcal{Y}$ and $\mathcal{D}^e := \{x_i^e, y_i^e\}_{i\in[n_e]} \overset{i.i.d}{\sim} \mathrm{P}^e$ with $[k] := \{1, ..., k\}$ for any $k \in \mathbb{Z}^+$. Our goal is to learn a robust predictor $f : \mathcal{X} \rightarrow \mathcal{Y}$ that only exploit the causal factor for prediction and generalize well to all domains $\mathcal{E} \supset \mathcal{E}_{\text{train}}$. We use respectively upper, lower case letter and Cursive letter to denote the random variable, the instance and the space, *e.g.*, a is an instance in the space $\mathcal{A}$ of random variable A. For $\mathcal{A} := f(\mathcal{X}) \cap \mathcal{B}$ with $\mathcal{B} := \mathbb{R}^p[i_1] \times \mathbb{R}^p[i_2] \times ... \times \mathbb{R}^p[i_k]$, the $[f(x)]_{\mathcal{A}}$ denotes the $f(x)$ restricted on dimensions of $\mathcal{A}$, *i.e.*, $[f(x)]_{\mathcal{A}} := [f_{i_1}(x), ..., f_{i_k}(x)]$. The Sobolev space $W^{k,p}(\mathcal{A})$ contains all f such that $\int_{\mathcal{A}} \left|\partial_A f^\alpha|_{A=a}\right|^p d\mu(a) < \infty, \forall \alpha \leq k$.

Structural Causal Model. The structural causal model (SCM) is defined as a triplet $M := \langle G, \mathcal{F}, P(\varepsilon)\rangle$, in which **i)** the causal structure $G := (V, E)$ (V, E respectively denote the node and edge set) is described by a directed acyclic graph (DAG); **ii)** the structural equations $\mathcal{F} := \{f_k\}_{V_k\in V}$ are autonomous, *i.e.*, intervening on V_k does not affect others, based on which we can define the *do*-operator and calculate the causal effect; **iii)** the $P(\varepsilon)$ are probability measure for exogenous variables $\{\varepsilon_k\}_k$. By assuming independence among $\{\varepsilon_k\}_k$, we obtain according to *Causal Markov Condition* that each P that is compatible with G has $\mathrm{P}(\{V_k = v_k\}_{V_k\in V}) = \Pi_k \mathrm{P}(V_k = v_k|Pa(k) = pa(k))$. An acyclic directed mixed graph (ADMG) can further allow the existence of bidirectional arrows $\leftrightarrow$, meaning the spurious correlation between two variables connected.

4 Methodology

We first incorporate the causal assumptions into LaCIM in sec. 4.1. Under such assumptions, we identify the invariant distributions $P(X|S, Z)$ and $P(Y|S)$, which are repectively dubbed as *generative invariance* and *causal invariance* that are robust to domain shifts. Equipped with these invariances, we in sec. 4.2 show that the causal factor can be identified without mixing information from non-causal one during prediction. Finally, we introduce our learning method in sec. 4.3 to estimate the $P(X|S, Z)$ and $P(Y|S)$, which are respectively resorted in the inference and prediction that constitute a robust predictor during test stage.

4.1 Latent Causal Invariance Models

In this section, we introduce a set of structural causal models dubbed as **La**tent **C**ausal **I**nvariance **M**odel (LaCIM), which incorporates the causal assumptions mentioned above and also the source of distributional shifts. The corresponding causal structure of LaCIM is illustrated in Fig. 1 (c), which we will introduce step-by-step from the skeleton in Fig. 1 (a).

Fig. 1 (a). Specifically, the ADMG in Fig. 1 (a) introduces latent factors $V := \{S, Z\}$ to model the abstractions/concepts that generate the observed variables (X, Y), as similarly assumed in

unsupervised latent generative models [37] for image generation. Further, we explicitly separate the V into S and Z, with only S causally related to the label Y. In image classification, such a causal factor refers to the (shape,contour) of the object need to be classified; while the image X is additionally affected by contextual factor such as *light, view*.

Fig. 1 (a) → Fig. 1 (b). In addition, we assume that S is spuriously correlated with Z, as marked by the red "↔" in Fig. 1 (a). Such a spurious correlation corresponds to the bias inherited from data, *e.g.* the contextual information in image classification. Therefore, the magnitude of this correlation is distribution-dependent and thus can vary across domains. Statistically, the "spurious correlation" implicates the presence of a third unobserved (we use dot circle to represent unobserved variables) confounder, which is denoted as C in Fig. 1 (b). The unblocked path from Z to Y induced by C can lead to learning the non-causal factor during data-fitting, which can degrade the performance on unseen domains if the correlation between this non-causal factor and the output is broken.

Fig. 1 (b) → Fig. 1 (c). Taking a further inspection in Fig. 1 (b), the varying degree of correlation can be either due to the distributional shift of $S, Z|C$ or of the C itself across domains (we use red color to mean varied distributions). As both shifts are domain-dependent, we in Fig. 1 (c) ascribe them to a domain variable D, which causes the mutation of its children nodes' distribution, *i.e.*, S, Z and C. Such a domain variable has been similarly introduced in [69, 68] to generate mutable variables. In our scenario, we do not require D to be observed; rather, we only need the domain index $\tilde{d}^e$ (one-hot encoded vector with length $m := |\mathcal{E}_{\text{train}}|$). The set of SCMs augmented with D, with the SCM Markovian compatible to the DAG of C, S, Z, X, Y in Fig. 1 (c), is dubbed as **La**tent **C**ausal **I**nvariance **M**odels (LaCIM) that is formally defined as follows:

Definition 4.1 (LaCIM)**.** *The LaCIM denotes a set of SCMs augmented with the domain variable D,* i.e., *$\{\langle M^e, d^e\rangle\}_{e\in\mathcal{E}}$, in which d^e denotes the value of D and $M^e := \langle G, \mathcal{F}^e, P(\varepsilon)\rangle$ for e. The G denotes the DAG restricted on C, S, Z, X, Y. For each environment/domain e, the $\mathcal{F}^e := \{f_x, f_y, f_s^e, f_z^e, f_c^e\}$ correspond to generating mechanism of X, Y, S, Z, C, with $f_c^e(\varepsilon_c) := g_c(\varepsilon_c, d^e)$, $f_s^e(c, \varepsilon_s) := g_s(c, \varepsilon_s, d^e)$ and $f_z^e(c, \varepsilon_z) := g_z(c, \varepsilon_z, d^e)$ from some g_c, g_s, g_z.*

Remark 1. *Different from scenarios in which X generates [28] nor generated from Y [1], we consider the scenario when the X and Y are generated concurrently, which can widely exist but ignored in the literature. For example, the clinicians are recording the disease status while implementing the ultrasound test at the same time, during medical diagnosis.*

As an illustration, we consider the following example, in which the distributional shifts caused by domain variable D can refer to sampling bias in data.

Example 4.1 (Sampling Bias)**.** *Consider the cat/dog classification, in which the animal in each image is either associated with the snow or grass. The D refers to the sampler, which generates the C that denotes time and weather to collect each sample. The S, Z respectively refer to the features of animals and context. Since each sampler may have a fixed sampling pattern (*e.g. *gets used to going out in the sunny morning (or in the snowy evening)), the data one collects may have sampling bias: dogs (cats) more associated with grass (snow) in the sunny morning (or snowy evening).*

The Def. 4.1 specifies the generating mechanisms across environments and how they differ. Equipped with such a specification, we can identify the invariant mechanisms that are stable to domain shifts:

Proposition 4.2 (Causal Invariance & Generative Invariance)**.** *For LaCIM in Def. 4.1, the $P(Y|S)$ and $P(X|S, Z)$ are invariant to shifts across $\mathcal{E}$, and are respectively denoted as **C**ausal **I**nvariance (CI) and **G**enerative **I**nvariance (GI).*

Remark 2. *The generating process from latent variables to observed variables follows from physical law,* e.g., *the shape, contour, color, view, light should satisfy physical constraints to generate a reasonable image. Therefore, it is naturally hold that such generating processes are invariant.*

The $P(X|S, Z)$ and $P(Y|S)$ can induce an invariant predicting mechanism. Specifically, for a new sample $x \leftarrow f_x(s^\star, z^\star, \varepsilon_x)$, $y \leftarrow f_y(s^\star, \varepsilon_y)$, we can first infer the causal factor $s^\star$ from $p_{f_x}(x|s, z)$ by maximizing log-likelihood of $p_{f_x}(x|s, z)$ over $\mathcal{S} \times \mathcal{Z}$ and then feed the estimated s into $p_{f_y}(y|s^\star)$ for prediction. To ensure the robustness of such a two-step invariant prediction, we need to answer two following *identifiability* questions:

1. *Can the inferred causal factor S not mix the information of (disentangled from) others?*
2. *Can such an invariant predictor recover the ground-truth predictor $P(Y|s^\star)$?*

We will answer these questions in the subsequent section, followed by our learning methods to identify the causal factor and the causal/generative invariance for prediction.

4.2 Identifiability Analysis

We present the identifiability results regarding **(i)** the disentanglement of inferred causal factor S from non-causal Z, and **(ii)** the induced true predicting mechanism $P(Y|s^\star)$ for $x \leftarrow f_x(s^\star, z^\star, \varepsilon_x)$, which respectively echo the two questions imposed in the last section.

Our main results are presented in theorem 4.4. To distinguish the causal factor S from others, our results require that the degree of diversity of S-Z correlation across environments is large enough, which has been similarly assumed in the literature of identifiability [52, 1]. Such a *diversity* condition implies the dramatical change of correlation between Z and Y, thus providing a clue to disentangle the S. Such a disentanglement analysis, is crucial to causal prediction but is ignored in existing literature about identifiability, such as those identifying the discrete latent confounders [32, 62], or those relying on *Additive Noise Model* (ANM) assumption [31], or linear Independent Component Analysis (ICA) [14, 35, 36, 75] (Please refer to supplement D.1 for more exhaustive reviews). More importantly, we will later in theorem 4.5 show the extension of above analysis from exponential family of $P(S, Z|C)$ to Sobelev space; and from ANM for Y to categorical distribution for Y.

We assume the ANM for $f_x(s, z, \varepsilon_x) = \hat{f}_x(s, z) + \varepsilon_x$ (we replace $\hat{f}_x$ with f_x for simplicity), which has been widely adopted to identify the causal factor [30, 54, 35]. We assume the f_x to be bijective and invertible (we will discuss it later). We first narrow our interest to a subset of LaCIM denoted as $\mathcal{P}_{\text{exp}}$ in which any model in $\mathcal{P}_{\text{exp}}$ satisfies that **(i)** the S, Z belong to the exponential family; and **(ii)** the Y is generated from the ANM:

$$\mathcal{P}_{\text{exp}} = \Big\{\text{LaCIM with any } m > 0 |\ y = f_y(s) + \varepsilon_y, p^e(s, z|c) := \Pi_{t=s,z} p_{\mathbf{T}^t, \mathbf{\Gamma}^t_{c,d^e}}(t|c), \forall e\Big\}, \text{with}$$

$$p_{\mathbf{T}^t, \mathbf{\Gamma}^t_{c,d^e}}(t) = \prod_{i=1}^{q_t} \exp\Big(\sum_{j=1}^{k_t} T^t_{i,j}(t_i)\Gamma^t_{c,d^e,i,j} + B_i(t_i) - A^t_{c,d^e,i}\Big), \forall k_t, q_t \tag{1}$$

for $t = s, z$ and $e \in \mathcal{E}$, with q_t, k_t respectively denoting the dimension of $t = s, z$ and the number of natural parameters in each dimension. The $\{T^t_{i,j}(t_i)\}$, $\{\Gamma^t_{c,d^e,i,j}\}$ denote the sufficient statistics and natural parameters, $\{B_i\}$ and $\{A^t_{c,d^e,i}\}$ denote the base measures and normalizing constants to ensure the integral of distribution equals to 1. Let $\mathbf{T}^t(t) := [\mathbf{T}^t_1(t_1), ..., \mathbf{T}^t_{q_t}(t_{q_t})] \in \mathbb{R}^{k_t \times q_t}$ $\big(\mathbf{T}^t_i(t_i) := [T^t_{i,1}(t_i), ..., T^t_{i,k_t}(t_i)], \forall i \in [q_t]\big)$, $\mathbf{\Gamma}^t_{c,d^e} := \big[\mathbf{\Gamma}^t_{c,d^e,1}, ..., \mathbf{\Gamma}^t_{c,d^e,q_t}\big] \in \mathbb{R}^{k_t \times q_t}$ $\big(\mathbf{\Gamma}^t_{c,d^e,i} := [\Gamma^t_{c,d^e,i,1}, ..., \Gamma^t_{c,d^e,i,k_t}], \forall i \in [q_t]\big)$. We further assume that the $P^e(C)$ serves to discrete distributions on the set $\{c_1, ..., c_R\}$, with which the $p^e(s, z) := \int p(s|c)p(z|c)dP^e(c) = \sum_r p^e(s, z|c_r)p^e(c_r)$ can be regarded as the mixture of exponential family distributions. Rather than uniquely inference, we target on disentangling the S from Z and also recovering the ground-truth predictor, which is formally defined as $\sim_{\text{exp}}$-identifiability as follows:

Definition 4.3 ($\sim_{\text{exp}}$-identifiability)**.** *Suppose the $\mathcal{X} \supseteq f_x(\mathcal{S} \times \mathcal{Z})$. We define a binary relation $\theta \sim_{\text{exp}} \tilde{\theta}$ on the parameter space of $\mathcal{X} \times \mathcal{Y}$: there exist two sets of permutation matrices and vectors, (M_s, a_s) and (M_z, a_z) for s and z respectively, such that for any $(x, y) \in \mathcal{X} \times \mathcal{Y}$, the following hold:*

$$\tilde{\mathbf{T}}^s([\tilde{f}_x^{-1}]_{\mathcal{S}}(x)) = M_s \mathbf{T}^s([f_x^{-1}]_{\mathcal{S}}(x)) + a_s, \tilde{\mathbf{T}}^z([\tilde{f}_x^{-1}]_{\mathcal{Z}}(x)) = M_z \mathbf{T}^z([f_x^{-1}]_{\mathcal{Z}}(x)) + a_z; \tag{2}$$

$$p_{\tilde{f}_y}(y|[\tilde{f}_x^{-1}]_{\mathcal{S}}(x)) = p_{f_y}(y|[f_x^{-1}]_{\mathcal{S}}(x)). \tag{3}$$

We then say that θ is $\sim_{\text{exp}}$-identifiable, if for any $\tilde{\theta}$, $p^e_\theta(x, y) = p^e_{\tilde{\theta}}(x, y)\ \forall e \in \mathcal{E}_{\text{train}}$, implies $\theta \sim_{\text{exp}} \tilde{\theta}$.

This definition is inspired by but beyond the scope of unsupervised scenario considered in nonlinear ICA [27, 35] in that, the former further disentangle S from Z (in Eq. (2)) and identify the true predicting mechanism (in Eq. (3)). To see disentanglement, note that for any clean (noise-free) sample $x \leftarrow f_x(s^\star, z^\star)$, the Eq. (2) ensures that the inferred causal factor $\tilde{\mathbf{T}}^s([\tilde{f}_x^{-1}]_{\mathcal{S}}(x))$ does *not* mix the information of others, unless the extreme case that there is a deterministic function between S and Z, in which it is impossible for S to be identified. With such an identification of s, the Eq. (3) further guarantees that the learned $p_{\tilde{f}_y}(y|[\tilde{f}^{-1}]_{\mathcal{S}}(x))$ can recover the ground-truth prediction probability density, *i.e.*, $p_{f_y}(y|[f_x^{-1}]_{\mathcal{S}}(x)) = p_{f_y}(y|s^\star)$. With noise, the $s^\star$ can be inferred with some indeterminacy. The formal result is presented in theorem 4.4.

Theorem 4.4 ($\sim_{\text{exp}}$-identifiability)**.** *For θ of $\mathcal{P}_{\text{exp}}$ in Def. 4.1 with $m := |\mathcal{E}_{\text{train}}|$, we have that the θ is $\sim_{\text{exp}}$ identifiable under following assumptions:*

1. *The characteristic functions of $\varepsilon_x, \varepsilon_y$ are almost everywhere nonzero.*
2. *f_x, f_x', f_x'' are continuous and f_x, f_y are bijective;*
3. *The $\{T_{i,j}^t\}_{1\le j\le k_t}$ are linearly independent in $\mathcal{S}$ or $\mathcal{Z}$ for each $i \in [q_t]$ for any $t = s, z$; and $T_{i,j}^t$ are twice differentiable for any $t = s, z, i \in [q_t], j \in [k_t]$;*
4. *The $\{\left(\mathbf{T}^s([f^{-1}]_{\mathcal{S}}(x)), \mathbf{T}^z([f^{-1}]_{\mathcal{Z}}(x))\right); \mathcal{B}(x) > 0\}$ contains a non-empty open set in $\mathbb{R}^{q_s\times k_s+q_z\times k_z}$, with $\mathcal{B}(x) := \prod_{i_s\in[q_s]} B_{i_s}([f^{-1}]_{i_s}(x)) \prod_{i_z\in[q_z]} B_{i_z}([f^{-1}]_{i_z}(x))$.*
5. *The $L := [P^{e_1}(C)^\top, ..., P^{e_m}(C)^\top]^\top \in \mathbb{R}^{m\times R}$ and $\left[[\mathbf{\Gamma}_{c_2,d^{e_1}}^{t=s,z} - \mathbf{\Gamma}_{c_1,d^{e_1}}^{t=s,z}]^\top, ..., [\mathbf{\Gamma}_{c_R,d^{e_m}}^{t=s,z} - \mathbf{\Gamma}_{c_1,d^{e_1}}^{t=s,z}]^\top\right]^\top \in \mathbb{R}^{(R\times m)\times(q_t\times k_t)}$ have full column rank.*

The assumptions 1-3 are trivial and easy to satisfy. The characteristics functions of $\varepsilon_x, \varepsilon_y$ can be almost everywhere non-zero for most continuous variables, such as Gaussian, exponential, beta, gamma distribution. This assumption can ensure the identifiability of $p(f^{-1}(x)$, as will be shown in the appendix. The bijectivity of f_x and f_y have been widely assumed in [30, 54, 53, 35, 75] as a basic condition for identifiability. It naturally holds for f_x to be bijective since it has been empirically proven in auto-encoder [38] that the low-dimension embeddings (*i.e.*, $q_s + q_z < q_x$) can recover the original input well and also that the variational auto-encoder can extract meaningful representations from x. For the θ with categorical Y such that $p(y = k|s) = [f_y]_k(s)/\left(\sum_k [f_y]_k(s)\right)$, the f_y may not satisfy the bijectivity condition. We will shown identifiability for such a categorical case later in theorem 4.5. The assumption 3 can be uniformly satisfied for all distributions in the strongly exponential family. The containment of an open set in assumption (4) for $\{\left(\mathbf{T}^s([f^{-1}]_{\mathcal{S}}(x)), \mathbf{T}^z([f^{-1}]_{\mathcal{Z}}(x))\right); \mathcal{B}(x) > 0\}$ implies that space expanded by sufficient statistics are dense in some open set, as a sufficient condition for the mixture distribution $P^e(C)$ and also $P^e(X, Y|c)$ to be identified. The diversity assumption (5) implies that **i)** $m \ge R$ and $m * R \ge \max(k_z * q_z, k_s * q_s) + 1$; and that **ii)** different environments are diverse enough in terms of S-Z correlation, as an almost a necessary for the invariant one to be identified (a different version is assumed in [1]). In supplement B.2, we will show that the **ii)** can hold unless the space of $\mathbf{\Gamma}$ belong to a zero-(Lebesgue) measure set. As indicated by the formulation, a larger m would be easier to satisfy the condition, which agrees with the intuition that more environments can provide more complementary information. Besides, our result can be extended to non-independent case among $\{s_1, ..., s_{q_s}\}$ (or $\{z_1, ..., z_{q_z}\}$), *i.e.*, $p_{\mathbf{T}^t,\mathbf{\Gamma}_{c,d^e}^t}(t) = \exp(\langle \mathbf{T}^t(t), \mathbf{\Gamma}_{c,d^e}^t\rangle + B(t) - A_{c,d^e}^t)$ $(t = s, z)$, which will shown in supplement B.2.

Extension to the general forms of LaCIM. We extend to general forms of LaCIM in theorem 4.5 as long as its $\mathrm{P}(S, Z|C = c) \in W^{r,2}(\mathcal{S} \times \mathcal{Z})$ (for some $r \ge 2$) and categorical Y, in the following theorem. This is accomplished by proving that any model in LaCIM can be approximated by a sequence of distributions with parameterization in $\mathcal{P}_{\text{exp}}$, motivated by [3] that the exponential family is dense in the set of distributions with bounded support, and in [44] that the continuous variable with multinomial logit model can be approximated by a series of distributions with *i.i.d* Gumbel noise as the temperature converges to infinity. The proof is left in the supplement.

Theorem 4.5 (Asymptotic $\sim_{\text{exp}}$-identifiability)**.** *Suppose the LaCIM satisfy that $p(x|s, z)$ and $p(y|s)$ are smooth w.r.t s, z and s respectively. For each e and $c \in \mathcal{C}$, suppose $P^e(S, Z|c) \in W^{r,2}(\mathcal{S}\times\mathcal{Z})$ for some $r \ge 2$, we have that the LaCIM is asymptotically $\sim_{\text{exp}}$-identifiable: $\forall\epsilon > 0$, $\exists$ $\sim_{\text{exp}}$-identifiable $\tilde{P}_\theta \in \mathcal{P}_{\text{exp}}$, s.t. $d_{\text{Pok}}(p^e(X, Y), \tilde{p}_\theta^e(X, Y)) < \epsilon, \forall e \in \mathcal{E}_{\text{train}}$* [3].

Our proof is built on [3] that any probability in Sobolev space can be approximated by a sequence of distribution with the number of natural paramters going to infinity, *i.e.*, $k_t \to \infty$.

4.3 Learning and Inference

Guided by the identifiability result, we propose to learn $P(X|S, Z)$ and $P(Y|S)$ via generative modeling following from Fig. 1 (c). Then to predict the label for a new sample x generated from $(s^\star, z^\star)$, we first leverage the learned $p(x|s, z)$ to infer $s^\star$ that is ensured to be able to not mix the non-causal information, followed by learned $P(y|\tilde{s}^\star)$ for prediction.

[3] The $d_{\text{Pok}}(\mu_1, \mu_2)$ denotes the Pokorov distance between μ_1 and μ_2, with $\lim_{n\to\infty} d_{\text{Pok}}(\mu_n, \mu) \to 0 \iff \mu_n \xrightarrow{d} \mu$.

4.3.1 Learning Method

To learn the $P(X|S,Z), P(Y|S)$ for invariant prediction, we reformulate the objective function of Variational Auto-Encoder (VAE) in the supervised scenario, in order to fit $\{p^e(x,y)\}_{e\in\mathcal{E}_{\text{train}}}$. As a latent generative model, the VAE was originally proposed for unsupervised generation from latent variables V to high-dimensional input variable X. To make such a generation tractable, the VAE introduced a variational distribution q_ψ parameterized by ψ to approximate the intractable posterior by maximizing the following **E**vidence **L**ower **Bo**und (ELBO): $-\mathcal{L}_{\theta,\psi} = \mathbb{E}_{p(x)}\left[\mathbb{E}_{q_\psi(v|x)} \log \frac{p_\theta(x,v)}{q_\psi(v|x)}\right] \leq \mathbb{E}_{p(x)}[\log p_\theta(x)]$, where the equality is achieved when $q_\psi(v|x) = p_\theta(v|x)$. Therefore, maximizing the ELBO over p_θ and q_ψ will drive **(i)** $q_\psi(v|x)$ to approximate $p_\theta(v|x)$; **(ii)** p_θ to estimate the ground-truth model p.

To adapt the above surrogate loss to our DAG in Fig. 1 (c), we introduce the variational distribution $q^e_\psi(s,z|x,y)$ for each environment e. The corresponding ELBO for e is

$$-\mathcal{L}^e_{\theta,\psi} \triangleq \mathbb{E}_{p^e(x,y)}\big[\mathbb{E}_{q^e_\psi(s,z|x,y)} \log \frac{p^e_\theta(x,y,s,z)}{q^e_\psi(s,z|x,y)}\big], \text{ where } p^e_\theta(x,y,s,z) = p_\theta(x|s,z)p_\theta(y|s)p^e(s,z).$$

Similarly, minimizing $\mathcal{L}^e_{\theta,\psi}$ can drive $p_\theta(x|s,z), p_\theta(y|s)$ to approximate the $p(x|s,z), p(y|s)$, and also $q^e_\psi(s,z|x,y)$ to estimate $p^e_\theta(s,z|x,y)$. Therefore, the q_ψ can inherit the properties of p_θ. As $p^e_\theta(s,z|x,y) = \frac{p^e_\theta(s,z|x)p_\theta(y|s)}{p^e_\theta(y|x)}$ for our DAG in Fig. 1 (c), we can similarly reparameterize $q^e_\psi(s,z|x,y)$ as $\frac{q^e_\psi(s,z|x)p_\theta(y|s)}{q^e_\psi(y|x)}$ with $q_\psi(y|s)$ replaced by $p_\theta(y|s)$ (since the goal of q_ψ is to mimic the behavior of p_θ). Then, the $\mathcal{L}^e_{\theta,\psi}$ can be rewritten as:

$$\mathcal{L}^e_{\theta,\psi} = \mathbb{E}_{p^e(x,y)}\Big[-\log q^e_\psi(y|x) - \mathbb{E}_{q^e_\psi(s,z|x)} \frac{p_\theta(y|s)}{q^e_\psi(y|x)} \log \frac{p_\theta(x|s,z)p^e_\theta(s,z)}{q^e_\psi(s,z|x)}\Big], \tag{4}$$

where $q^e_\psi(y|x) = \int_{\mathcal{S}} q^e_\psi(s|x)p_\theta(y|s)ds$. We correspondingly parameterize the prior model $p^e_\theta(s,z)$ and inference model $q^e_\psi(s,z|x)$ as $p_\theta(s,z|\tilde{d}^e)$ and $q_\psi(s,z|x,\tilde{d}^e)$, in which $\tilde{d}^e$ (of environment e) denotes the domain *index* that can be represented by the one-hot encoded vector with length $m := |\mathcal{E}_{\text{train}}|$. The overall loss function is:

$$\mathcal{L}_{\theta,\psi} \triangleq \sum_{e\in\mathcal{E}_{\text{train}}} \mathcal{L}^e_{\theta,\psi}. \tag{5}$$

The training datasets $\{\mathcal{D}^e\}_{e\in\mathcal{E}_{\text{train}}}$ are applied to optimize the prior models $\{p(s,z|\tilde{d}^e)\}_e$, inference models $\{q_\psi(s,z|x,\tilde{d}^e)\}_e$, generative model $p_\theta(x|s,z)$ and predictive model $p_\theta(y|s)$. Particularly, the parameters of $p_\theta(x|s,z)$ and $p_\theta(y|s)$ are shared among all environments, motivated by the the invariance property of $P(X|S,Z)$ and $P(Y|S)$ across all domains.

4.3.2 Inference & Prediction.

We leverage the learned $P(X|S,Z), P(Y|S)$ for prediction. According to Prop. 4.2 and Eq. (3) in theorem 4.4, the induced predictor via $P(X|S,Z), P(Y|S)$ can recover the true predicting mechanism for any distributional shifts from $\mathcal{E}$. Specifically, for any x generated by $(s^\star, z^\star)$, we first optimize the following log-likelihood of $p_\theta(x|s,z)$ over $\mathcal{S}\times\mathcal{Z}$ to infer $s^\star, z^\star$,

$$\max_{s,z} \log p_\theta(x|s,z) + \lambda_s\|s\|_2^2 + \lambda_z\|z\|_2^2, \tag{6}$$

with hyperparameters $\lambda_s > 0$ and $\lambda_z > 0$ in order to control the learned s, z in a reasonable scale. Note that Eq. Eq. (6) is different from the maximum a posterior estimation since the posterior $q^e_\psi(s,z|x)$ is parameterized differently for different e while the $p_\theta(x|s,z)$ is invariantly parameterized for $\mathcal{E}$ (this is because $p(x|s,z)$ is invariant). For optimization, we adopt the strategy in [61] that first sample some candidate points from $\mathcal{N}(0,I)$ and select the optimal one in terms of Eq. (6) as initial point; then use Adam to optimize for another T iterations. The implementation details and optimization effect are shown in supplement E.2. Finally, with estimated $\tilde{s}^\star, \tilde{z}^\star$, we implement the learned $p_\theta(y|\tilde{s}^\star)$ for prediction: $\tilde{y} := \arg\max_y p_\theta(y|\tilde{s}^\star)$.

5 Experiments

We first verify the identifiability claims of theorem 4.4 in sec. 5.1. Then we evaluate LaCIM on real-world data in sec. 5.2: Non-I.I.D. Image dataset with Contexts (NICO); Colored MNIST (CMNIST); Alzheimer's Disease Neuroimaging Initiative (ADNI `www.loni.ucla.edu/ADNI` for early prediction of Alzheimer's Disease), to verify the generalization ability of our method on the target domain with distributional shifts.

5.1 Simulation

To verify the identifiability claims, we implement LaCIM on synthetic data. We generate C, S, Z, X, Y following Fig. 1 (with details left in supplementary). We choose $m = 3, 5$ with the same total number of samples. To verify the advantage of learning on multiple diverse domains ($m > 1$), we compare with pool-LaCIM: minimizing the loss Eq. (4) on the pooled data from all m domains. We compute the mean correlation coefficient (MCC) adopted in [35], which measures the goodness of identifiability under permutation by introducing cost optimization to assign each learned component to the source component. We run all methods for 100 times, with the average recorded in Fig. 2a. The superiority of LaCIM over pool-LaCIM, together with the fact that LaICM with $m = 5$ performs better than $m = 3$, verify the benefit of more domains to satisfy the diversity condition. To illustrate the learning effect, we visualize the learned Z (with S left in supplement E.1) in Fig. 2b.

Method	MCC for Z	MCC for S
pool-LaCIM	0.41	0.71
LaCIM (**Ours**, $m = 3$)	0.63	**0.84**
LaCIM (**Ours**, $m = 5$)	**0.71**	**0.84**

(a) Mean Correlation Coefficient for S and Z.

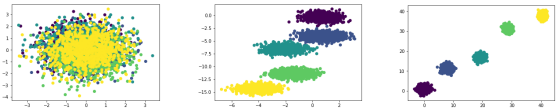

(i) pool-LaCIM (ii) LaCIM (iii) $p_{\theta^\star}(z|D)$

(b) Estimated posteriors ((i),(ii)) and the ground-truth ((iii)).

Figure 2: Identification of Latent Variables. As shown qualitatively (b) and quantitatively (a), the LaCIM can identify the latent variables (up to permutation and point-wise transformation).

5.2 Real-world Data

We verify the generalization ability of LaCIM on three data: NICO, CMNIST and ADNI.

Dataset. We describe the datasets as follows (X, Y denotes the input and output; D is unobserved):

- *NICO*. We consider the cat/dog classification in "Animal" dataset in NICO, a benchmark for non-i.i.d problem in [20]. Each animal is associated with "grass","snow" contexts. The D denotes the attributes of the sampler. The C denotes the time and weather of sampling, which generates the S, Z that respectively denote the semantic and contextual features. We split the dataset into m training domains and the test domain, in which each domain has different proportions of contexts associated with each animal, *i.e.*, (%cat in grass, %cat in snow, %dog in grass, %dog in snow), due to different sampling strategies determined by D. The proportion vectors of all domains are introduced in Tab. 3. The distributional shift refers to the spurious correlation between the context and the label.
- *CMNIST*: We relabel the digits 0-4 and 5-9 as $y = 0$ and $y = 1$, based on MNIST. Then we color p^e $(1 - p^e)$ of images with $y = 0$ $(y = 1)$ as green and others as red. We set $m = 2$ with $p^{e_1} = 0.95, p^{e_2} = 0.99$; while the $p^{e_{\text{test}}}$ for the test domain is set to 0.1. The D denotes the attributes of the painter. The Z, S respectively represent the features related to the color and the digit. Their confounder C denotes the time and weather for which the painter D draws the number and color, *e.g.*, the painter tends to draw red 0 more often than green 1 in the sunny morning. In this regard, the distributional shift refers to the spurious correlation between the color and the label.
- *ADNI*. The $\mathcal{Y} := \{0, 1, 2\}$, with 0,1,2 respectively denoting Normal Control, Mild Cognitive Impairment and AD. The X is structural Magnetic resonance imaging. We split the data into $m = 2$ training domains and the test domain, with different values of D that denotes Age, TAU (a biomarker [24]). The C, S (Z) respectively denote the hormone level that

affects the brain structure development and the disease-related (-unrelated) brain regions. The distributional shifts among all domains are due to different values of D.

Compared Baselines & Implementation Details. We compare with (i) Empirical Risk Mnimization from $X \to Y$ (ERM), (ii) domain-adversarial neural network (DANN) [15], (iii) Maximum Mean Discrepancy with Adversarial Auto-Encoder (MMD-AAE) [43], (iv) Domain Invariant Variational Autoencoders (DIVA) [29], (v) Invariant Risk Mnimization (IRM) [1], (vi) Supervised VAE (sVAE): our LaCIM implemented by VAE without disentangling S, Z. For all methods, the network structures of $q_\psi^e(s, z|x)$, $p_\theta(x|s, z)$ and $p_\theta(y|s)$ for CMNIST, NICO and ADNI are shared (details introduced in supplement E.4, E.5, E.6, Tab. 7, 8). We implement SGD as optimizer, with learning rate (lr) 0.5 and weight decay (wd) $1e$-5 for CMNIST; lr 0.01 with decaying $0.2\times$ every 60 epochs, wd $5e$-5 for NICO and ADNI (wd is $2e$-4). The batch-size are set to 256, 30 and 4 for CMNIST, NICO, ADNI.

Table 1: Accuracy (%) on test domain. Average over 10 runs.

Method \ Dataset	NICO				CMNIST		ADNI ($m = 2$)		
	$m = 8$		$m = 14$		$m = 2$		D: Age	D: TAU	# Params
	ACC	# Params	ACC	# Params	ACC	# Params	ACC	ACC	
ERM	60.3 ± 2.8	18.08M	59.3 ± 2.1	18.08M	91.9 ± 0.9	1.12M	62.1 ± 3.2	64.3 ± 1.0	28.27M
DANN	58.9 ± 1.7	19.13M	60.1 ± 2.6	26.49M	84.8 ± 0.7	1.1M	61.0 ± 1.5	65.2 ± 1.1	30.21M
MMD-AAE	60.8 ± 3.4	19.70M	64.8 ± 7.7	19.70M	92.5 ± 0.8	1.23M	60.3 ± 2.2	65.2 ± 1.5	36.68M
DIVA	58.8 ± 3.4	14.86M	58.1 ± 1.4	14.87M	86.1 ± 1.0	1.69M	61.8 ± 1.8	64.8 ± 0.8	33.22M
IRM	61.4 ± 3.8	18.08M	62.8 ± 4.6	18.08M	92.9 ± 1.2	1.12M	62.2 ± 2.6	65.2 ± 1.1	28.27M
sVAE	60.4 ± 2.1	18.25M	64.3 ± 1.2	19.70M	93.6 ± 0.9	0.92M	62.7 ± 2.5	66.6 ± 0.8	37.78M
LaCIM (**Ours**)	$\mathbf{63.2 \pm 1.7}$	18.25M	$\mathbf{66.4 \pm 2.2}$	19.70M	$\mathbf{96.6 \pm 0.3}$	0.92M	$\mathbf{63.8 \pm 1.1}$	$\mathbf{67.3 \pm 0.9}$	37.78M

Main Results & Discussions. We report accuracy over 10 runs for each method. As shown in Tab. 1, our LaCIM consistently outperforms others on all data. Specifically, the advantage over IRM and ERM may due to the incorporation of causal assumptions embedded in Fig. 1 (c). Further, the improvement over sVAE is benefited from the separation of S from others to avoid spurious correlation. Besides, a larger m (with the total sample size fixed) can bring further benefit on NICO, which may due to the easier satisfaction of the diversity condition in theorem 4.4.

Interpretability. We visualize the learned S and Z on CMNIST and NICO. Specifically, for CMNIST, we visualize the generated image (with only digit "0" among all classes that belong to $Y = 0$ and digit "7" among all classes that belong to $Y = 1$) by interpolating S (and Z) with fixed Z (and S); for NICO, we adopt the gradient method [67], which visualizes the derivatives of the $S^\star$ (*i.e.*, dimension of S that has the highest correlation with Y) with respect to each image.

As shown in Fig. 3a, the generated sequential images in the 1st and 2nd row look more like "7" from "0" as s increases; while the sequential images in the 2nd-row change from red to green as z increases. Besides, different dimensions of S can learn different differentiating semantic information. For example, the first dimension can learn to add the dash in the hand-writing "7"; while the second dimension can learn to remove the left part of "0" to "7" as interpolated. For the dimension of Z, it learned other non-differentiating factors such as width, color. This result reflects that the learned S and Z correspond to the digit (causal factor of Y) and color-related features. For NICO, Fig. 3b shows the ability of identifying more explainable semantic features of LaCIM than ERM in which the learned features can mix the background information. Supplement E.5 provides more results.

6 Conclusions & Discussions

We propose recovering *latent causal factor* that is robust to distributional shifts caused by a domain variable. We introduce the causal and non-causal latent factors that are spuriously correlated with each other, and generate the input and the output via invariant mechanisms. Under this invariance, the causal factor is guaranteed to be disentangled from the non-causal one, which induces the ground-truth predictor that holds on all domains. A reformulated generative model is proposed for inferring the causal factor and prediction. A possible drawback of our model lies in our requirement of the number of environments for identifiability, the relaxation of which is left in future work.

Generation with interpolated S with Z fixed

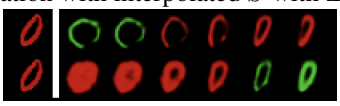

Generation with interpolated Z with S fixed

(a) Visualization on CMNIST

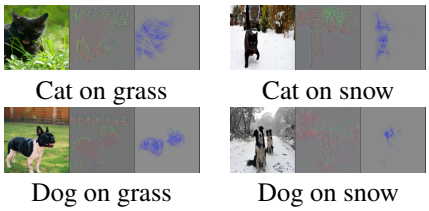

(b) Visualization on NICO

Figure 3: (a) Visualization on CMNIST via interpolation. (b) Visualization on NICO via gradient [67]. From the left to right: original image, ERM and LaCIM.

Broader Impact

We claim that this work does not present any foreseeable negative social impact.

References

[1] Martin Arjovsky, Léon Bottou, Ishaan Gulrajani, and David Lopez-Paz. Invariant risk minimization. *arXiv preprint arXiv:1907.02893*, 2019.

[2] O Barndorff-Nielsen. Identifiability of mixtures of exponential families. *Journal of Mathematical Analysis and Applications*, 12(1):115–121, 1965.

[3] Andrew R Barron and Chyong-Hwa Sheu. Approximation of density functions by sequences of exponential families. *The Annals of Statistics*, pages 1347–1369, 1991.

[4] Alexis Bellot and Mihaela van der Schaar. Generalization and invariances in the presence of unobserved confounding. *arXiv preprint arXiv:2007.10653*, 2020.

[5] Shai Ben-David, John Blitzer, Koby Crammer, and Fernando Pereira. Analysis of representations for domain adaptation. In *Advances in neural information processing systems*, pages 137–144, 2007.

[6] Aharon Ben-Tal, Laurent El Ghaoui, and Arkadi Nemirovski. *Robust optimization*, volume 28. Princeton University Press, 2009.

[7] Yoshua Bengio. The consciousness prior. *arXiv preprint arXiv:1709.08568*, 2017.

[8] Yoshua Bengio, Aaron Courville, and Pascal Vincent. Representation learning: A review and new perspectives. *IEEE Transactions on Pattern Analysis and Machine Intelligence*, 35(8):1798–1828, 2013.

[9] Irving Biederman. Recognition-by-components: a theory of human image understanding. *Psychological review*, 94(2):115, 1987.

[10] Peter Bühlmann. Invariance, causality and robustness. *arXiv preprint arXiv:1812.08233*, 2018.

[11] Krzysztof Chalupka, Pietro Perona, and Frederick Eberhardt. Visual causal feature learning. *arXiv preprint arXiv:1412.2309*, 2014.

[12] Mike Davies. Identifiability issues in noisy ica. *IEEE Signal processing letters*, 11(5):470–473, 2004.

[13] Christian Döbler et al. Stein's method of exchangeable pairs for the beta distribution and generalizations. *Electronic Journal of Probability*, 20, 2015.

[14] Jan Eriksson and Visa Koivunen. Identifiability and separability of linear ica models revisited. In *Proc. of ICA*, volume 2003, pages 23–27, 2003.

[15] Yaroslav Ganin, Evgeniya Ustinova, Hana Ajakan, Pascal Germain, Hugo Larochelle, François Laviolette, Mario Marchand, and Victor Lempitsky. Domain-adversarial training of neural networks. *Journal of Machine Learning Research*, 17:1–35, 2016.

[16] Leon A. Gatys, Alexander S. Ecker, and Matthias Bethge. A neural algorithm of artistic style. *Journal of Vision*, 2015.

[17] Mingming Gong, Kun Zhang, Tongliang Liu, Dacheng Tao, Clark Glymour, and Bernhard Schölkopf. Domain adaptation with conditional transferable components. In *International Conference on Machine Learning*, pages 2839–2848, 2016.

[18] Patrick J Grother. Nist special database 19 handprinted forms and characters database. *National Institute of Standards and Technology*, 1995.

[19] Rita Guerreiro and Jose Bras. The age factor in Alzheimer's disease. *Genome medicine*, 7(1):106, 2015.

[20] Yue He, Zheyan Shen, and Peng Cui. Towards non-iid image classification: A dataset and baselines. *Pattern Recognition*, 110:107383, 2020.

[21] Christina Heinze-Deml and Nicolai Meinshausen. Conditional variance penalties and domain shift robustness. *Machine Learning*, pages 1–46, 2020.

[22] Patrik Hoyer, Dominik Janzing, Joris M Mooij, Jonas Peters, and Bernhard Schölkopf. Nonlinear causal discovery with additive noise models. *Advances in neural information processing systems*, 21:689–696, 2008.

[23] Jiayuan Huang, Arthur Gretton, Karsten Borgwardt, Bernhard Schölkopf, and Alex J Smola. Correcting sample selection bias by unlabeled data. In *Advances in Neural Information Processing Systems*, pages 601–608, 2007.

[24] Christian Humpel and Tanja Hochstrasser. Cerebrospinal fluid and blood biomarkers in Alzheimer's disease. *World journal of psychiatry*, 1(1):8, 2011.

[25] Aapo Hyvarinen and Hiroshi Morioka. Unsupervised feature extraction by time-contrastive learning and nonlinear ica. In *Advances in Neural Information Processing Systems*, pages 3765–3773, 2016.

[26] Aapo Hyvärinen and Petteri Pajunen. Nonlinear independent component analysis: Existence and uniqueness results. *Neural Networks*, 12(3):429–439, 1999.

[27] Aapo Hyvärinen, Hiroaki Sasaki, and Richard Turner. Nonlinear ICA using auxiliary variables and generalized contrastive learning. In *The 22nd International Conference on Artificial Intelligence and Statistics*, pages 859–868, 2019.

[28] Maximilian Ilse, Jakub M Tomczak, and Patrick Forré. Designing data augmentation for simulating interventions. *arXiv preprint arXiv:2005.01856*, 2020.

[29] Maximilian Ilse, Jakub M Tomczak, Christos Louizos, and Max Welling. DIVA: Domain invariant variational autoencoders. *arXiv preprint arXiv:1905.10427*, 2019.

[30] D Janzing, J Peters, JM Mooij, and B Schölkopf. Identifying confounders using additive noise models. In *Proceedings of the 25th Conference on Uncertainty in Artificial Intelligence (UAI 2009)*, pages 249–257. AUAI Press, 2009.

[31] Dominik Janzing, Jonas Peters, Joris Mooij, and Bernhard Schölkopf. Identifying confounders using additive noise models. *arXiv preprint arXiv:1205.2640*, 2012.

[32] Dominik Janzing, Eleni Sgouritsa, Oliver Stegle, Jonas Peters, and Bernhard Schölkopf. Detecting low-complexity unobserved causes. *arXiv preprint arXiv:1202.3737*, 2012.

[33] Fredrik D Johansson, David Sontag, and Rajesh Ranganath. Support and invertibility in domain-invariant representations. In *The 22nd International Conference on Artificial Intelligence and Statistics*, pages 527–536, 2019.

[34] Guoliang Kang, Xuanyi Dong, Liang Zheng, and Yi Yang. Patchshuffle regularization. *arXiv preprint arXiv:1707.07103*, 2017.

[35] Ilyes Khemakhem, Diederik Kingma, Ricardo Monti, and Aapo Hyvarinen. Variational autoencoders and nonlinear ica: A unifying framework. In *International Conference on Artificial Intelligence and Statistics*, pages 2207–2217. PMLR, 2020.

[36] Ilyes Khemakhem, Ricardo Monti, Diederik Kingma, and Aapo Hyvarinen. Ice-beem: Identifiable conditional energy-based deep models based on nonlinear ica. *Advances in Neural Information Processing Systems*, 33, 2020.

[37] Diederik P Kingma and Max Welling. Auto-encoding variational Bayes. In *Proceedings of the International Conference on Learning Representations (ICLR 2014)*, Banff, Canada, 2014. ICLR Committee.

[38] Mark A Kramer. Nonlinear principal component analysis using autoassociative neural networks. *AIChE journal*, 37(2):233–243, 1991.

[39] David Krueger, Ethan Caballero, Joern-Henrik Jacobsen, Amy Zhang, Jonathan Binas, Remi Le Priol, and Aaron Courville. Out-of-distribution generalization via risk extrapolation (rex). *arXiv preprint arXiv:2003.00688*, 2020.

[40] Kun Kuang, Peng Cui, Susan Athey, Ruoxuan Xiong, and Bo Li. Stable prediction across unknown environments. In *Proceedings of the 24th ACM SIGKDD International Conference on Knowledge Discovery & Data Mining*, pages 1617–1626, 2018.

[41] Ciarán M Lee, Christopher Hart, Jonathan G Richens, and Saurabh Johri. Leveraging directed causal discovery to detect latent common causes. *arXiv preprint arXiv:1910.10174*, 2019.

[42] Da Li, Yongxin Yang, Yi-Zhe Song, and Timothy Hospedales. Learning to generalize: Meta-learning for domain generalization. In *Proceedings of the AAAI Conference on Artificial Intelligence*, volume 32, 2018.

[43] Haoliang Li, Sinno Jialin Pan, Shiqi Wang, and Alex C Kot. Domain generalization with adversarial feature learning. In *Proceedings of the IEEE Conference on Computer Vision and Pattern Recognition*, pages 5400–5409, 2018.

[44] Chris J Maddison, Andriy Mnih, and Yee Whye Teh. The concrete distribution: A continuous relaxation of discrete random variables. *arXiv preprint arXiv:1611.00712*, 2016.

[45] Aleksander Madry, Aleksandar Makelov, Ludwig Schmidt, Dimitris Tsipras, and Adrian Vladu. Towards deep learning models resistant to adversarial attacks. *arXiv preprint arXiv:1706.06083*, 2017.

[46] Sara Magliacane, Thijs van Ommen, Tom Claassen, Stephan Bongers, Philip Versteeg, and Joris M Mooij. Domain adaptation by using causal inference to predict invariant conditional distributions. In *Advances in Neural Information Processing Systems*, pages 10846–10856, 2018.

[47] Diego Marcos, Michele Volpi, and Devis Tuia. Learning rotation invariant convolutional filters for texture classification. In *2016 23rd International Conference on Pattern Recognition (ICPR)*, pages 2012–2017. IEEE, 2016.

[48] James A Mortimer. Brain reserve and the clinical expression of Alzheimer's disease. *Geriatrics (Basel, Switzerland)*, 52:S50–3, 1997.

[49] Krikamol Muandet, David Balduzzi, and Bernhard Schölkopf. Domain generalization via invariant feature representation. In *International Conference on Machine Learning*, pages 10–18, 2013.

[50] Sinno Jialin Pan, Ivor W Tsang, James T Kwok, and Qiang Yang. Domain adaptation via transfer component analysis. *IEEE Transactions on Neural Networks*, 22(2):199–210, 2010.

[51] Judea Pearl. *Causality*. Cambridge university press, 2009.

[52] Jonas Peters, Peter Bühlmann, and Nicolai Meinshausen. Causal inference by using invariant prediction: identification and confidence intervals. *Journal of the Royal Statistical Society: Series B (Statistical Methodology)*, 78(5):947–1012, 2016.

[53] Jonas Peters, Dominik Janzing, and Bernhard Schölkopf. *Elements of causal inference: foundations and learning algorithms*. MIT press, 2017.

[54] Jonas Peters, Joris M Mooij, Dominik Janzing, and Bernhard Schölkopf. Causal discovery with continuous additive noise models. *Journal of Machine Learning Research*, 15(1):2009–2053, 2014.

[55] Mateo Rojas-Carulla, Bernhard Schölkopf, Richard Turner, and Jonas Peters. Invariant models for causal transfer learning. *The Journal of Machine Learning Research*, 19(1):1309–1342, 2018.

[56] Jan-Willem Romeijn and Jon Williamson. Intervention and identifiability in latent variable modelling. *Minds and machines*, 28(2):243–264, 2018.

[57] Andreas Rossler, Davide Cozzolino, Luisa Verdoliva, Christian Riess, Justus Thies, and Matthias Nießner. Faceforensics++: Learning to detect manipulated facial images. In *Proceedings of the IEEE International Conference on Computer Vision*, pages 1–11, 2019.

[58] Shiori Sagawa, Pang Wei Koh, Tatsunori B Hashimoto, and Percy Liang. Distributionally robust neural networks for group shifts: On the importance of regularization for worst-case generalization. *arXiv preprint arXiv:1911.08731*, 2019.

[59] Bernhard Schölkopf. Causality for machine learning. *arXiv preprint arXiv:1911.10500*, 2019.

[60] Bernhard Schölkopf, Dominik Janzing, Jonas Peters, and Kun Zhang. Robust learning via cause-effect models. *arXiv preprint arXiv:1112.2738*, 2011.

[61] Lukas Schott, Jonas Rauber, Matthias Bethge, and Wieland Brendel. Towards the first adversarially robust neural network model on mnist. *arXiv preprint arXiv:1805.09190*, 2018.

[62] Eleni Sgouritsa, Dominik Janzing, Jonas Peters, and Bernhard Schölkopf. Identifying finite mixtures of nonparametric product distributions and causal inference of confounders. In *Proceedings of the 29th Conference on Uncertainty in Artificial Intelligence (UAI 2013)*, pages 556–575. AUAI Press, 2013.

[63] Shiv Shankar, Vihari Piratla, Soumen Chakrabarti, Siddhartha Chaudhuri, Preethi Jyothi, and Sunita Sarawagi. Generalizing across domains via cross-gradient training. In *Proceedings of the International Conference on Learning Representations (ICLR 2018)*, 2018.

[64] Shohei Shimizu, Patrik O Hoyer, and Aapo Hyvärinen. Estimation of linear non-gaussian acyclic models for latent factors. *Neurocomputing*, 72(7-9):2024–2027, 2009.

[65] Connor Shorten and Taghi M Khoshgoftaar. A survey on image data augmentation for deep learning. *Journal of Big Data*, 6(1):60, 2019.

[66] Ricardo Silva, Richard Scheine, Clark Glymour, and Peter Spirtes. Learning the structure of linear latent variable models. *Journal of Machine Learning Research*, 7(Feb):191–246, 2006.

[67] Karen Simonyan, Andrea Vedaldi, and Andrew Zisserman. Deep inside convolutional networks: Visualising image classification models and saliency maps. *arXiv preprint arXiv:1312.6034*, 2013.

[68] Adarsh Subbaswamy and Suchi Saria. I-spec: An end-to-end framework for learning transportable, shift-stable models. *arXiv preprint arXiv:2002.08948*, 2020.

[69] Adarsh Subbaswamy, Peter Schulam, and Suchi Saria. Preventing failures due to dataset shift: Learning predictive models that transport. In *The 22nd International Conference on Artificial Intelligence and Statistics*, pages 3118–3127. PMLR, 2019.

[70] Masashi Sugiyama, Taiji Suzuki, Shinichi Nakajima, Hisashi Kashima, Paul von Bünau, and Motoaki Kawanabe. Direct importance estimation for covariate shift adaptation. *Annals of the Institute of Statistical Mathematics*, 60(4):699–746, 2008.

[71] Raphael Suter, Djordje Miladinovic, Bernhard Schölkopf, and Stefan Bauer. Robustly disentangled causal mechanisms: Validating deep representations for interventional robustness. In *International Conference on Machine Learning*, pages 6056–6065, 2019.

[72] M. Tan and Quoc V. Le. Efficientnet: Rethinking model scaling for convolutional neural networks. *arXiv preprint, arXiv:1905.11946*, 2019.

[73] Luke Taylor and Geoff Nitschke. Improving deep learning using generic data augmentation. *arXiv preprint arXiv:1708.06020*, 2017.

[74] Damien Teney, Ehsan Abbasnejad, and Anton van den Hengel. Unshuffling data for improved generalization. *arXiv preprint arXiv:2002.11894*, 2020.

[75] Takeshi Teshima, Issei Sato, and Masashi Sugiyama. Few-shot domain adaptation by causal mechanism transfer. *arXiv preprint arXiv:2002.03497*, 2020.

[76] Jose Vina and Ana Lloret. Why women have more Alzheimer's disease than men: gender and mitochondrial toxicity of amyloid-β peptide. *Journal of Alzheimer's disease*, 20(s2):S527–S533, 2010.

[77] Daniel E Worrall, Stephan J Garbin, Daniyar Turmukhambetov, and Gabriel J Brostow. Harmonic networks: Deep translation and rotation equivariance. In *Proceedings of the IEEE Conference on Computer Vision and Pattern Recognition*, pages 5028–5037, 2017.

[78] Chuanlong Xie, Fei Chen, Yue Liu, and Zhenguo Li. Risk variance penalization: From distributional robustness to causality. *arXiv preprint arXiv:2006.07544*, 2020.

[79] Chiyuan Zhang, Samy Bengio, Moritz Hardt, Benjamin Recht, and Oriol Vinyals. Understanding deep learning requires rethinking generalization. *arXiv preprint arXiv:1611.03530*, 2016.

[80] Kun Zhang, Biwei Huang, Jiji Zhang, Clark Glymour, and Bernhard Schölkopf. Causal discovery from nonstationary/heterogeneous data: Skeleton estimation and orientation determination. In *IJCAI: Proceedings of the Conference*, volume 2017, page 1347. NIH Public Access, 2017.

[81] Kun Zhang, Bernhard Schölkopf, Krikamol Muandet, and Zhikun Wang. Domain adaptation under target and conditional shift. In *International Conference on Machine Learning*, pages 819–827, 2013.

[82] Han Zhao, Remi Tachet des Combes, Kun Zhang, and Geoffrey J Gordon. On learning invariant representation for domain adaptation. *arXiv preprint arXiv:1901.09453*, 2019.